International Journal of Biological Macromolecules 281 (2024) 136222

Contents lists available at ScienceDirect

International Journal of Biological Macromolecules

journal homepage: www.elsevier.com/locate/ijbiomac

Interactions of biofilm polysaccharides produced by human infective bacteria with molecules of the quorum sensing system. A microscopy and NMR study

Barbara Bellich [a,1,2], Michele Cacioppo [b,2,3], Rita De Zorzi [b], Roberto Rizzo [c], John W. Brady [d], Paola Cescutti [c,*]

[a] Advanced Translational Diagnostics Laboratory, Institute for Maternal and Child Health-IRCCS "Burlo Garofolo", Via dell'Istria 65/1, 34137 Trieste, Italy
[b] Department of Chemical and Pharmaceutical Sciences, INSTM UdR Trieste, University of Trieste, Via Licio Giorgieri 1, 34127 Trieste, Italy
[c] Department of Life Sciences, Bld C11 University of Trieste, Via Licio Giorgieri 1, 34127 Trieste, Italy
[d] Food Science Department, Cornell University, 101A Stocking Hall, Ithaca, NY 14853, USA

ARTICLE INFO

Keywords:
Polysaccharides
Klebsiella pneumoniae
Burkholderia
Quorum sensing
TEM
AFM
NMR

ABSTRACT

Biofilms are the most common lifestyle adopted by bacterial communities where cells live embedded in a self-produced hydrated matrix. Although polysaccharides are considered essential for matrix architecture, their possible functional roles are still rather unexplored. The primary structure of polysaccharides produced by *Klebsiella pneumoniae* and species of the *Burkholderia cepacia* Complex revealed a composition rich in rhamnose. The methyl group on carbon 6 of rhamnose units lowers the polymer hydrophilicity and can form low polarity regions on the polysaccharide chains. These regions promote chain-chain interactions that contribute to the biofilm matrix stability, but may also act as binding sites for low-polarity molecules, aiding their mobility through the hydrated matrix. In particular, quorum sensing system components crucial for the biofilm life cycle often display poor solubility in water. Therefore, *cis*-11-methyl-2-dodecenoic acid and L-homoserine-lactones were investigated by NMR spectroscopy for their possible interaction with polysaccharides. In addition, the macromolecular morphology of the polysaccharides was assessed using atomic force and electron microscopies to define the role of Rha residues on the three-dimensional conformation of the polymer. NMR data revealed that quorum sensing components interact with Rhamnose-rich polysaccharides, and the extent of interaction depends on the specific primary structure of each polysaccharide.

1. Introduction

Nowadays, microbiologists consider the "biofilm community" the most common way of life for bacteria [1–3]. This association of bacteria embedded in a self-produced matrix may include bacteria from single or multiple species. Biofilms (BF) offer several advantages to bacteria, such as protection from various threats, accumulation of suitable nutrients, and, due to cell proximity, biochemical synergy, as well as cell-cell communication. The latter function is mediated by molecules of the so-called "quorum sensing" system (QS), also known as autoinducers. The QS system allows bacteria to collectively modify their behaviour in response to changes in cell density and species composition of their close surroundings [4].

The overall biofilm architecture is shaped by the presence of the extracellular matrix [5,6], a complex system composed mainly of macromolecules (polysaccharides (PS), proteins, and extra-cellular DNA) which provides an entangled scaffold of gel-like appearance able to host bacteria and low molecular mass chemical species. The precise architecture of the matrix is not known but, due to the compositional diversity of macromolecules produced by different bacteria, it is likely

* Corresponding author at: Department of Life Sciences, University of Trieste, via L. Giorgieri 1, Bdg C11, 34127 Trieste, Italy.
E-mail address: pcescutti@units.it (P. Cescutti).

[1] Barbara Bellich performed the experiments while working at the Department of Life Sciences, University of Trieste, *Via* Licio Giorgieri 1, Bdg. C11, 34,127 Trieste, Italy.

[2] B. Bellich and M. Cacioppo equally contributed to this work.

[3] Present address: Department of Biological, Chemical and Pharmaceutical Sciences and Technologies (STEBICEF), University of Palermo, Viale delle Scienze, Ed. 17 - Stanislao Cannizzaro, 90,128 Palermo, Italy.

https://doi.org/10.1016/j.ijbiomac.2024.136222
Received 7 June 2024; Received in revised form 20 September 2024; Accepted 30 September 2024
Available online 1 October 2024

rather specific for each bacterial species. In fact, during our 20-year-long study of the structure of exopolysaccharides (EPOL) produced by species of the *Burkholderia cepacia* Complex, we found several different primary structures related to distinct bacterial species [6–9].

We believe that a detailed investigation of the BF matrix structure-function relationship could provide interesting hints for biofilm control, and possibly disruption, especially for those BFs produced by bacterial species associated with serious human infections, that are difficult to eradicate and are often associated with antibiotic resistance. Among these, species of the *Burkholderia cepacia* Complex and strains of *Klebsiella pneumoniae* are both involved in infections, particularly, but not only, in the lungs of immune-compromised and cystic fibrosis patients [11,12].

Recently, we determined the structure of the PS produced by *B. multivorans* strain C1576 (hereafter named EPOL C1576), which is characterized by a tetrasaccharide repeating unit composed of two mannose and two rhamnose residues, with one rhamnose 50 % *O*-methyl-substituted in position 3 (Scheme 1) [8]. This characteristic attracted our attention since Rha residues, 6-deoxy-sugars, are less polar than other more common sugars, like glucose. In addition, partial methylation in position 3 contributes to the non-polar character of the polymer. This feature is relevant because macromolecules forming the biofilm, although surrounded by an aqueous environment, must be insoluble in water in order to form stable contacts with each other and in synergy with other macromolecular components, that constitute the structural framework of the biofilm. It is also worth mentioning that low molecular mass chemical species like signalling molecules belonging to the QS system have low water solubility and might need assistance to move through the biofilm space to reach target cells.

Our previous work demonstrated that EPOL C1576 is indeed able to interact with fluorescent aromatic dyes, thus increasing their solubility in water, as indicated by the increased fluorescence intensity of the solution and by the broadening of NMR signals of the dye, due to a decreased transverse relaxation rate associated with the interaction with a high molecular mass polymeric species [13].

Besides the structural function in setting up the scaffold that includes and protects bacterial cells, we hypothesise that the biofilm matrix actively contributes to the biochemistry of the biofilm by interacting with bioactive molecules. Here, we investigate the interactions of EPOL C1576 with poorly water-soluble molecules of the quorum sensing system to validate the diffusion-helper role of the polymer. Besides EPOL C1576, we included two Rha-containing polysaccharides, whose primary structures have recently been investigated, showing a percentage of Rha even larger than in EPOL C1576: the EPOL produced by *B. cenocepacia* H111 (a *B. cepacia* Complex reference strain) [10] and the capsular polysaccharide (CPS) of *Klebsiella pneumoniae* strain Kp-B1 [14] (Scheme 1). The morphologies of EPOL C1576 both in the solid state and in solution have already been described using atomic force microscopy (AFM) and transmission electron microscopy (TEM) [15,16], while the morphologies of EPOL H111 and CPS KpB-1 are reported in this paper.

In particular, we focused on two types of autoinducers: *cis*-11-methyl-2-dodecenoic acid, which belongs to the Diffusible Signal Factor (DSF) family [17], and N-octanoyl-L-homoserine-lactone (AHL-8) (Scheme 2). Autoinducers accumulate in the environment as bacterial cell density increases, and their concentration is monitored by bacteria to follow cell number changes and to alter gene expression altogether. AHLs are the most common class of autoinducers in Gram-negative bacteria: they have in common a homoserine-lactone ring N-acylated with 4- to 18-carbon acyl chains [4]. DSF autoinducers control virulence and modulate the transitions between planktonic and biofilm-associated lifestyles [18]. Moreover, DSF is responsible for inducing a dispersion response of the native biofilm in several Gram-negative and Gram-positive bacteria [19].

The comparison of the interaction properties of the three polysaccharides with the QS molecules might better define the role of Rha-containing polysaccharides in these BF systems.

To investigate the influence of the length of the aliphatic tail on the interaction with polysaccharides, two additional homoserine-lactone derivatives have been tested: AHL-6 (with a shorter, six-carbon chain) and AHL-12 (with a longer, twelve-carbon chain).

2. Experimental

2.1. Bacteria strains, production and purification of polysaccharides

Burkholderia multivorans strain C1576 (LMG 16660) is a reference strain from the panel of *Burkholderia cepacia* Complex strains [20] and was purchased from BCCM™bacteria collection (Dept. of Biochemistry and Microbiology, Faculty of Sciences of Ghent University, Belgium). The *ΔbcsB*/pBerA strain [21], a kind gift of Prof. Tim T. Nielsen

1) EPOL C1576

[2)-α-D-Man*p*-(1→2)-α-D-Rha*p*-(1→3)-α-D-Rha*p*-(1→3)-α-D-Man*p*-(1→]$_n$

3

|

OCH_3 (50%)

2) EPOL H111-SOL

[2)-α-L-Rha*p*-(1→3)-α-L-[Rha*p* or Man*p*]-(1→3)-α-L-Rha*p*-(1→2)-α-L-Rha*p*-(1→]$_n$

(50%)

3) CPS KpB-1

[3)-α-D-Gal*p*A-(1→2)-α-L-Rha*p*-(1→2)-α-L-Rha*p*-(1→2)-α-L-Rha*p*-(1→3)-β-D-Gal*p*-(1→]$_n$

4

↑

1

α-L-Rha*p*

Scheme 1. Primary structures of the investigated polysaccharides repeating units. EPOL C1576 has 50 % of 2-Rha C3 substituted with a methyl group; EPOL H111-SOL presents 50 % replacement of the 3-α-L-Rha with a α-3-α-L-Man.

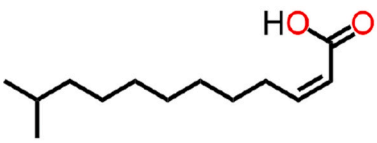

cis-11-methyl-2-dodecenoic acid

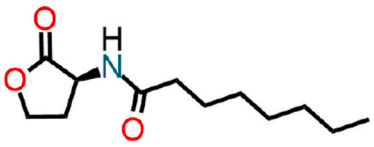

N-octanoyl-L-homoserine-lactone

Scheme 2. Structures of the investigated QS molecules.

(Costerton Biofilm Center, Department of Immunology and Microbiology, University of Copenhagen, DK-2200 Copenhagen, Denmark), was derived from *Burkholderia cenocepacia* H111, a clinical isolate from a cystic fibrosis patient [22], and was used for polysaccharide production. *Klebsiella pneumoniae* KpB-1 belongs to the Sequence Type 12 and was isolated from the pleural fluid of an inpatient admitted at an Italian hospital [14]. The culture conditions for the production and purification of polysaccharides from bacteria are described in the Supplementary file. ^{1}H NMR spectra of the obtained polysaccharides were recorded to check their purity.

2.2. AFM experiments

AFM analysis was performed in tapping (non-contact) mode on samples produced by the spray drying method. Diluted volumes (c.a. 100 μL) of PS solutions in different solvents or mixtures of solvents (5 μg/mL) were sprayed on mica substrate surfaces using a commercial airbrush. Before the analysis, samples were dried for 12 h at STP (Standard Temperature and Pressure conditions). AFM Images were acquired on a Nanoscope IIIa VEECO Instrument using an HQ:NSC19/AL_BS MikroMasch AFM tip and data were analysed using the Gwyddion v2.50 software.

2.3. TEM experiments

Samples were dispersed on 200-mesh copper grids (Electron Microscopy Sciences), previously prepared with a carbon layer, and stained with uranyl acetate (saturated solution). For each sample, 4 μL of a 5 μg/mL solution of the PS was deposited on an uncharged grid and dried overnight. The following day, a drop of uranyl acetate solution (3 μL) was deposited on the grid, incubated for 30 s, and dried with filter paper from the edge of the grid. The staining procedure was repeated twice. Grids were analysed on a Philips EM208 Transmission Electron Microscope (TEM) operating at 100 kV and images were acquired on a Quemesa camera (EMSIS), using the RADIUS software.

2.4. NMR investigation of the interactions between polysaccharides and Quorum Sensing molecules

A known amount of *cis*-11-methyl-2-dodecenoic acid (DSF) was dissolved in $CDCl_3$; a volume corresponding to 9.4 μmol ($9.4 \bullet 10^{-6}$ mol $\times$ 212.33 g$\bullet$mol^{-1} = 0.002 g *i.e.* 2 mg) was transferred in a glass vial and dried under nitrogen flux. The PS solution was prepared by dissolving an amount of polymer corresponding to 0.4 μmol of PS repeating unit in 0.7 mL of 99.9 % D_2O, followed by lyophilization. The procedure of re-dissolving in 99.9 % D_2O and lyophilizing the PS was repeated three times to suppress the residual HOD signal. The PS solution was then added to the dried DSF sample and left for 16 h at 25 °C, under stirring, to allow molecular interactions and the consequent increase in DSF solubilization. The sample was centrifuged at 14500 ×*g* for 10 min to eliminate undissolved DSF, and transferred into an NMR tube. In addition to the above-described polysaccharides, dextran (BioChemika Fluka, 670 KDa) was used as a negative control. Despite having α(1–6) linkages that grant a highly flexible structure, this homopolysaccharide was chosen because it is commercially available in different molecular mass ranges, very water soluble, lacks charged groups as well as low-polarity residues (*e.g.* rhamnose). Therefore, its highly polar character is expected to hamper strong interactions with apolar molecules. NMR spectra were recorded at 25 °C using a 500 MHz VARIAN spectrometer. The same procedure was applied also for AHL-6, AHL-8, and AHL-12 molecules except that they were dissolved in CD_3CD_2OD. Spectra were analysed using the MestreNova software.

3. Results and discussion

3.1. AFM and TEM investigation

The tendency of EPOL C1576 to assume a globular conformation was already demonstrated by AFM both in solid state and in solution, and it was observed that, upon increasing the polysaccharide concentration, the globules form aggregates [15,16]. This behaviour was traced back to intra- and inter-molecular non-polar interactions between pairs of rhamnose residues along the polysaccharide backbone (Scheme 1). The possible aggregation tendency of EPOL H111-SOL, which contains stretches of up to seven Rha, was investigated by AFM. In this analysis, the spray-drying technique was applied starting from solutions of the polysaccharide in three different solvents, to elucidate the effect of chemical environments with different polarity on the polymer morphology. As reported previously in the case of EPOL C1576, the aggregates observed by AFM on spray-dried samples are comparable to those obtained using the AFM technique in solution [16]. Interestingly, AFM images obtained from water solutions (Fig. 1A) show the occurrence of large linear aggregates, along with some isolated chains. These aggregates might form through the association of chains stranded in an elongated conformation along which "blobs" occur formed by either inter- or intra-chain entanglements. In fact, the profiling of elongated segments and blobs gives 0.42 nm and 1.5 nm values, respectively, and these figures are compatible with the thickness of a polysaccharide chain (0.42 nm) and chain entanglement (1.5 nm) [23,24].

AFM experiments carried out in 50 % water/methanol (Fig. 1B) and pure methanol (Fig. 1C) solutions still show PS aggregation; in fact, a mean value of 3.0 nm was recorded by profiling different objects detected in the images. However, neither elongated aggregates, as in Fig. 1A, nor a dispersion of single macromolecules were observed. Evidently, the abundance of Rha residues in the EPOL H111-SOL primary structure and the lack of strong polar groups (such as the carboxylate moieties present in CPS KpB-1) hamper the complete breakage of apolar interactions, thus maintaining some PS aggregation.

TEM images (Fig. 1D) were obtained from samples dried by blotting the microscope grid. This procedure was demonstrated to be equivalent to a slow drying of the sample [16]. The images obtained from EPOL H111-SOL did not evidence the presence of single macromolecules, but rather the occurrence of elongated aggregates, further bundled together side-by-side. Considering the differences between the AFM and TEM sample preparations, these structures confirm the evidence obtained by AFM for dry samples sprayed as water solutions onto a mica surface, where extended linear objects were detected.

The AFM images recorded from CPS KpB-1 samples obtained by spray-drying a water polysaccharide solution on a mica surface showed large objects, suggesting the presence of aggregates of more spherical objects of different sizes (Fig. 2A) with a profile evaluation yielding vertical dimensions of the spheres spanning from 3.5 to 4.5 nm. Moving

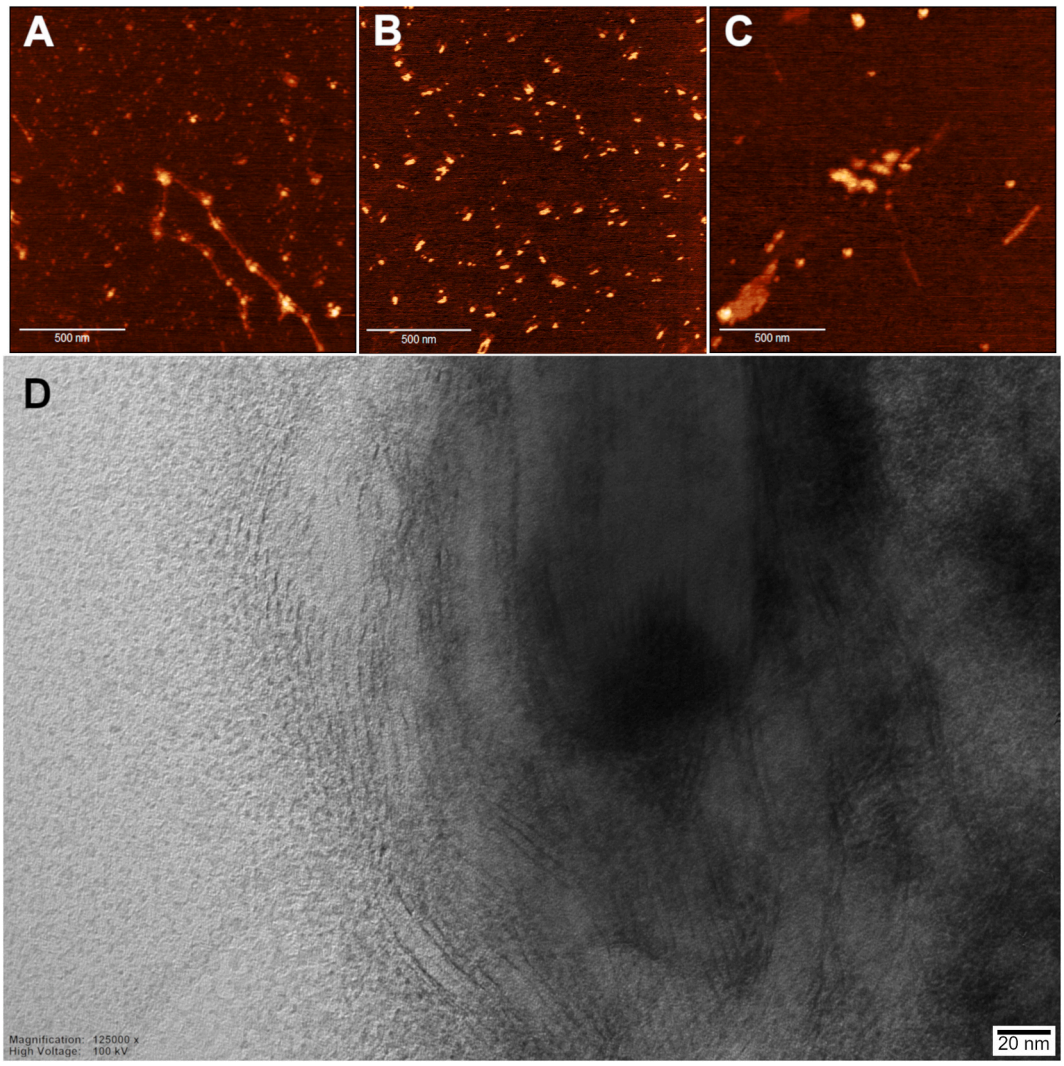

Fig. 1. AFM images of Epol H111-SOL obtained after spray-drying from water (A), water/methanol (B) and methanol (C) solutions on mica surface, (D) TEM image of Epol H111-SOL.

from water to water/methanol solutions, AFM images of spray-dried samples show a decrease in the aggregation tendency (Fig. 2B). In fact, besides a single larger aggregate, the majority of the sample presents a globular morphology and a small dimension indicative of the folding of individual macromolecules into spherical objects (Fig. 2B). Finally, AFM images of spray-dried methanol solutions of the polysaccharide show only small individual objects suggesting a low tendency of the macromolecules to aggregate (Fig. 2C) but still maintaining a spherical morphology with a mean diameter of 4.0 nm. Evidence points to the conclusion that the low polarity of methanol hampers the formation of chain-chain interactions by shielding the Rha residues. This polymer also contains one galacturonic acid residue (GalA) per repeating unit, conferring a negative charge to the polysaccharide backbone, thus further disfavouring the formation of aggregates.

TEM micrographs (Fig. 2) confirm the ability of this polysaccharide to form large aggregates of globular objects, probably constituted of single polymer chains folded in a spherical morphology (Fig. 2D). In addition, few isolated macromolecules can be detected (Fig. 2E) which, however, tend to form dimers, thus confirming the aggregation ability of the polymer.

In conclusion, AFM and TEM analyses confirm that all three polysaccharides investigated can form polymer aggregates due to the presence of low-polarity monosaccharides (Rha) along their primary structure. AFM experiments in less polar solvent systems (water/methanol or pure methanol), where polymer aggregates are partially or totally disrupted by the hydrophobic interactions between the methyl groups of rhamnose and methanol, confirm that the low polarity sequences do have a relevant role in aggregation.

3.2. Interaction of Quorum Sensing molecules with biofilm polysaccharides

The QS molecules investigated in this research work do not have chromophores which could be conveniently exploited by optical spectroscopies like UV–Vis, fluorescence, or circular dichroism, to study their interaction with the polysaccharides. Chemical modifications of their structures to introduce labels could result in interaction artefacts, especially considering the low molecular mass of the QS molecules. Therefore, to analyse the interaction of the QS molecules with polysaccharides, we resort to NMR spectroscopy, a technique already successfully employed to study the interactions between EPOL C1576 and aromatic dyes [13].

The increase in solubility of the QS species in water as a consequence of their interaction with polysaccharides was measured. Polysaccharide D_2O solutions were added to a known amount of solid QS species and allowed to interact overnight, before recording ^1H NMR spectra. A set of NMR signals assigned to protons of the QS molecules, and not superimposing with those of the polysaccharide, were selected to quantify the

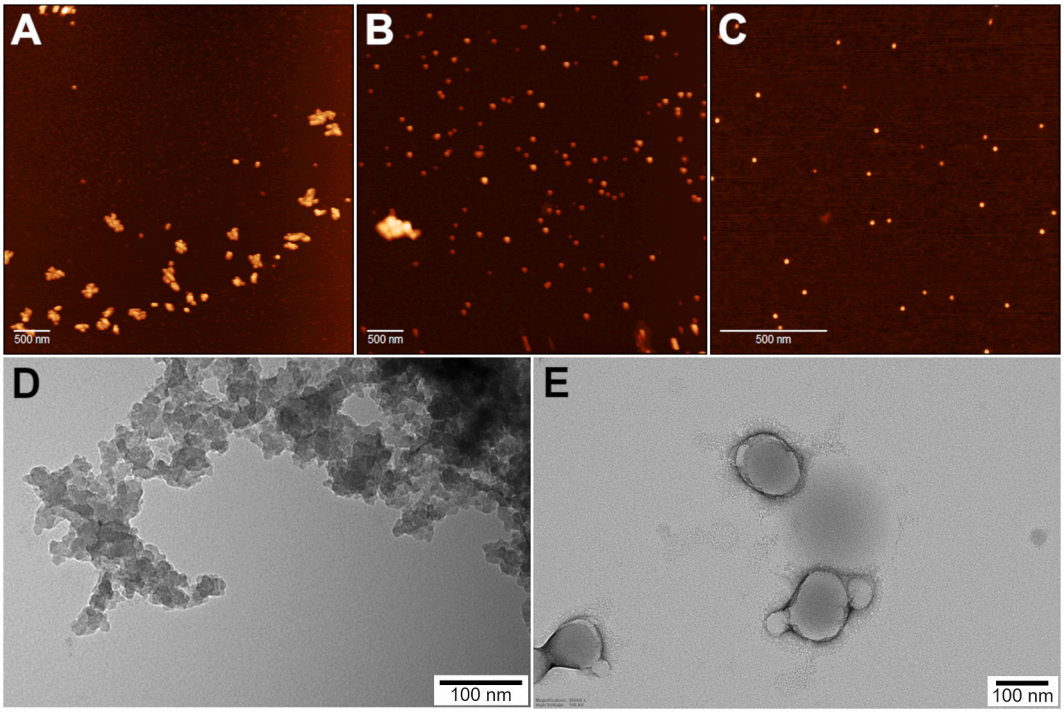

Fig. 2. AFM images of CPS KpB-1 obtained after spray-drying from water (A), water/methanol (B) and methanol (C) solutions on mica surface. TEM micrographs of CPS KpB-1. D) large aggregates, E) monomers and dimers.

amount of each QS molecule driven into solution by the presence of the PS. These signals were integrated relative to the area of the anomeric proton signals (H1) corresponding to one repeating unit of the PS. The comparison of the area ratios with those evaluated using the reference polysaccharide dextran allowed the detection of the increase in solubility of QS molecules in the aqueous phase. Dextran is a glucan with no low-polarity rhamnose sequences and, therefore, is not able to interact extensively with the QS species carrying them into the aqueous phase, as

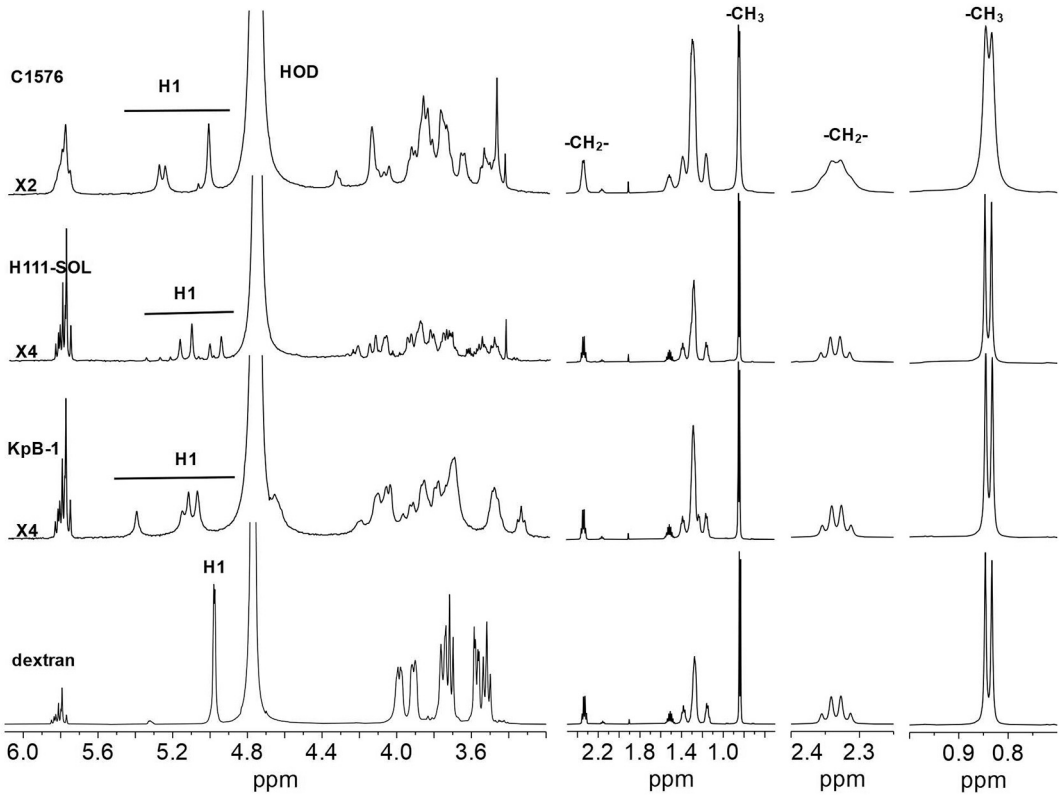

Fig. 3. ^{1}H NMR spectra of the investigated bacterial polysaccharides in the presence of the Diffusible Signal Factor (DSF). Enlargements of the -CH_2- and -CH_3 resonances are reported in the panels to the right.

already observed in the case of aromatic dyes and DSF [13].

The NMR spectra obtained for EPOL C1576, EPOL H111, CPS KbB-1, and dextran in the presence of DSF are reported in Fig. 3.

In the NMR spectrum of dextran (Fig. 3), the anomeric proton resonance signal of glucose is easily detected at 5.0 ppm. On the DSF side, the -CH_2- and -CH_3 protons resonances are recognised at 2.33 and 0.84 ppm, respectively. Since these signals do not overlap with PS proton resonances, they can be conveniently exploited to evaluate the relative concentration of DFS in water in the presence of different PS. The quantification of the relative concentration of DSF in the aqueous phase is evaluated by normalizing the integrated DSF signals to the anomeric H1 resonances, to relate it to one repeating unit of each polysaccharide.

The NMR spectrum obtained for DSF in the presence of EPOL C1576 is shown in Fig. 3. This spectrum is similar to that obtained in the presence of dextran but for the increased complexity of the anomeric resonances, reflecting the higher complexity of the EPOL C1576 repeating unit of four sugar residues (Scheme 1). Oligosaccharide repeating units are the characteristic structural feature of each individual PS (Scheme 1) and have different sizes for the polymers chosen for this study. To take this aspect into account in the evaluation of the DSF relative concentration in the aqueous phase in the presence of either of the two polysaccharides, dextran was considered as composed of a tetrasaccharide repeating unit of four identical Glc residues. A similar approach was also used for the two remaining polysaccharides, EPOL H111-SOL and CPS KpB-1. H111-SOL is described by an octasaccharide repeating unit, which is the smallest sequence including all sugar residues. To compare the amount of DSF solubilized in the presence of EPOL H111-SOL and CPS KpB-1, dextran was considered as composed of eight and six Glc residues, respectively. The integration of NMR resonances for the DSF-polysaccharide systems, together with their normalization to the DSF-dextran system, is reported in Table 1. These results show that the four PS contribute differently to the DSF solubilization. In particular, the DSF solubility in water in the presence of the investigated polysaccharides follows the ranking:

Dextran < CPS KpB-1 < EPOL C1576 < EPOL H111-SOL

We interpret the DSF solubility increase as assisted by non-polar interactions between the QS species and Rha-rich sequences of all polysaccharides except dextran. NMR data confirm poor interactions of DSF with dextran and, therefore, validate its use as a reference. In fact, the amount of DSF molecules in the dextran solution is lower than that present in the other PS solutions, as revealed by the peak integration ratio between selected resonances of DSF and PS moieties. A low solubility, slightly higher than the dextran reference, is observed when *K. pneumoniae* KpB-1 CPS is present in the solution. Actually, this polymer includes in its primary structure a galacturonic acid, whose interaction with the negative charge of the DSF molecule is expected to be repulsive, thus hampering a strong DSF-polymer interaction and, consequently, a significant increase in DSF water solubility. The highest solubility of DSF in D_2O is obtained in the presence of EPOL H111-SOL. In its repeating unit, this polymer contains up to seven Rha residues (Scheme 1), allowing for strong non-polar interaction with the DSF hydrophobic tail. EPOL C1576 contains only two Rha residues, separated by a pair of Man residues. As expected, EPOL C1576 interacts less strongly with DSF compared to EPOL H111-SOL, producing an increase in its D_2O solubility that is intermediate among the investigated polymers. In conclusion, the DSF solubility ranking reported above is nicely explained by considering the specificity of the primary structure of each polysaccharide.

It is worth noticing that the NMR signal of the -CH_2- (2.33 ppm) and -CH_3 (0.84 ppm) groups of the DSF molecule in the presence of the EPOL C1576 is characterized by a peak enlargement with relative loss of resolution, an effect that was not detected in the DSF spectra in the presence of the other investigated polysaccharides. This behaviour suggests that the interaction between the signal molecule and the polysaccharide directly involves the methyl groups whose dynamics assume the typical values of a large macromolecule.

A similar experiment performed using the QS molecule AHL-8 with the same polysaccharides (EPOL C1576, EPOL H111-SOL, CPS KbB-1, and dextran) yielded the spectra reported in Fig. 4 and the integration values in Table 2. The AHL-8 solubility was evaluated considering only the -CH_3 AHL signal at 0.84 ppm because it does not overlap with resonances attributed to the investigated PS. Considering signal integration and normalization, the ranking of AHL-8 water solubility in the presence of polysaccharides is:

Dextran < CPS KpB-1 < EPOL C1576 < EPOL H111

The AHL-8 solubility ranking is in line with the data obtained for DSF, confirming that the conclusions previously drawn hold for both QS molecules. The correlation between the solubility of the DSF and AHL-8 and the different structures of the three polysaccharides suggests an interesting active role of the Rha residues in biofilm biochemistry.

To elucidate the influence of the aliphatic tails of AHL molecules, NMR experiments were carried out using AHL-6 and AHL-12, revealing that the length of the AHL aliphatic chain plays a role in the interaction of the small molecule with the polysaccharide. Although AHL-6 is more soluble in water than AHL-8, the presence of Rha-containing polysaccharides further increases its solubility, as demonstrated by the comparison with the dextran-containing system. As in the previous cases, the ranking of polysaccharides increasing the solubility of AHL-6 follows the same order:

Dextran < CPS KpB-1 < EPOL C1576 < EPOL H111-SOL

However, when AHL-12 was tested, flocculation was observed only in the solution of the Rha-containing polysaccharides, indicating a large extent of aggregation between the polymers and AHL-12. Although the flocculation prevented NMR analysis of the interaction, the macroscopic behaviour of the system indicates the presence of an extended network of inter-crossed AHL-12 and polysaccharide molecules.

Table 1
Quantification of DSF solubilization induced by the presence of the investigated polysaccharides, through integration of selected ^1H resonances.

Polysaccharide	Anomeric[a] protons	-CH_2-[b] (2.33 ppm)	-CH_3[c] (0.84 ppm)	-CH_2- PS/ -CH_2- Dextran[d]	-CH_3 PS/ -CH_3 Dextran[e]
EPOL C1576	4	3.46	12.85	3.46	3.85
DEXTRAN	4	1.00	3.34		
EPOL H111-SOL	8	14.25	37.54	5.94	5.63
DEXTRAN	8	2.40	6.67		
CPS KpB-1	6	2.32	7.91	1.52	1.58
DEXTRAN	6	1.53	5.00		

[a] Number of anomeric protons in the polysaccharide repeating unit. For comparison with dextran, the same number of anomeric protons were used.
[b,c] Area integration values (with respect to the anomeric protons).
[d] Area ratio of -CH_2- resonance in each PS solution with respect to dextran.
[d,e] Area ratio of -CH_3 resonance in each PS solution with respect to dextran.

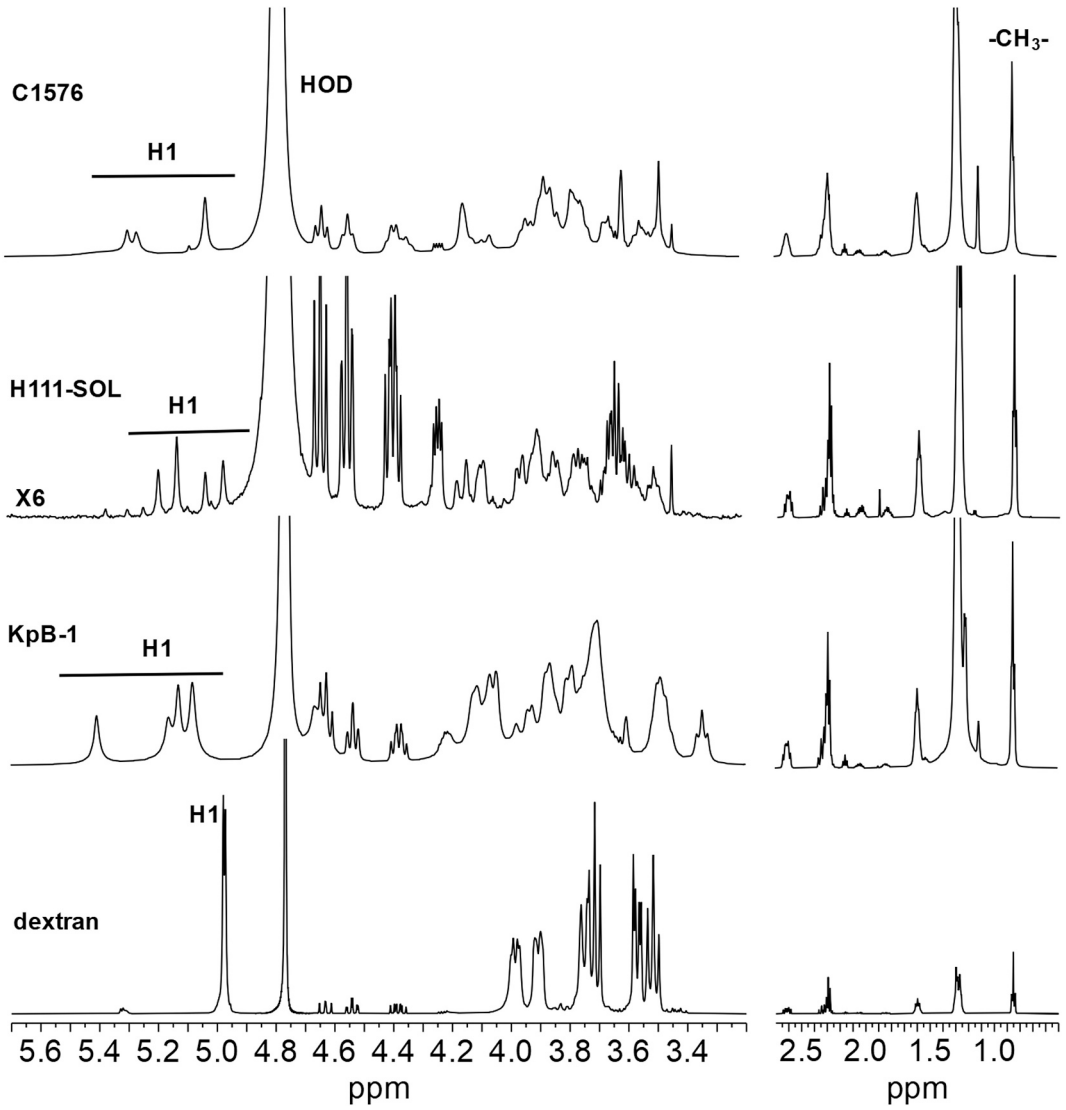

Fig. 4. ^{1}H NMR spectra of the investigated bacterial polysaccharides in the presence of the AHL-8.

Table 2
Quantification of AHL-6 and AHL-8 solubilization induced by the presence of the investigated polysaccharides, through integration of selected ^{1}H resonances.

		AHL-6		AHL-8	
Polysaccharide	Anomeric[a] protons	-CH_3[b] (0.84 ppm)	-CH_3 PS/ -CH_3 Dextran[c]	-CH_3[d] (0.84 ppm)	-CH_3 PS/ -CH_3 Dextran[e]
EPOL C1576	4	216.06	6.07	5.32	6.82
DEXTRAN	4	35.59		0.78	
EPOL H111-SOL	8	1102.97	15.49	58.59	37.32
DEXTRAN	8	71.19		1.57	
CPS KpB-1	6	111.63	2.09	2.28	1.95
DEXTRAN	6	53.39		1.17	

[a] Number of anomeric protons in the polysaccharide repeating unit. For comparison with dextran, the same number of anomeric protons were used.
[b] Area integration values of -CH_3 AHL-6 resonance (with respect to the anomeric protons).
[c] Area ratio of -CH_3 AHL-6 resonance in each PS solution with respect to dextran.
[d] Area integration values of -CH_3 AHL-8 resonance (with respect to the anomeric protons).
[e] Area ratio of -CH_3 AHL-8 resonance in each PS solution with respect to dextran.

4. Conclusions

Details on the possible roles of macromolecules composing biofilm matrices are not fully known. It is quite obvious that proteins may have roles as transport agents and enzymes and that extracellular DNA could contribute to horizontal gene transfer. However, polysaccharides are generally considered a purely structural component, contributing only to the setup of the water-swollen gel-like consistency of the biofilm and to maintaining bacterial cells in the biofilm domain. Nevertheless, the whole biofilm might be considered a "super-organism" where all its components have an active biological role, including the matrix and its constituents. In particular, it is worth mentioning that QS molecules, like

DSF and AHL included in the present study, are generally rather water-insoluble and, therefore, not particularly prone to move freely through the biofilm domain. Hence, they require assistance from biofilm components in their movement toward their targets.

During our investigation on the structure of polysaccharides produced by members of the *B. cepacia* Complex and *K. pneumoniae* species, we unravelled their Rha-rich primary structure. Since these monomers are less polar compared to common sugars of natural polysaccharides, we assumed that QS factors could loosely interact with the low-polarity Rha-sequences, thus travelling through the biofilm by moving along the polysaccharide backbone and/or exploiting the interconnected polysaccharide network spanning the whole biofilm, to jump between chains. The assumption is experimentally supported by the microscopy studies carried out on these polysaccharides. In fact, AFM and TEM experiments revealed that the polysaccharides aggregate in water solution indicating their preference for self-interacting over the possibility of extensive water solvation. These findings suggest that besides polar interactions, hydrophobic interactions involving polysaccharides may be established if they contain low-polarity sugar sequences, thus contributing to the architecture of the biofilm matrix.

The NMR data obtained in the present study nicely proved this assumption, suggesting a previously unknown active biological role of the polysaccharides composing biofilm matrices. In this kind of investigation, the diversity of polysaccharide chemical composition among bacteria is rooted in the optimal biofilm environment of each species and strongly connected to specific biological functions of the matrix.

The present study is based on purified PS from bacterial biofilms obtained *in vitro*, while *in vivo* matrices are a complex entanglement of different types of macromolecules interacting with each other and with the environment. The QS-PS interaction studied by NMR spectroscopy is far from the situation *in vivo*, but any new information about the components of the biofilm matrix contributes to a better understanding of their role and can thus lead to the development of new strategies to fight bacterial infections. The great variability of polysaccharides produced by different bacterial species, characterized by different primary structures and conformations, does not allow a generalization of their biological activities in biofilms. To better understand the biological role of polysaccharides in the biofilm matrix, specific studies for each bacterial species are required.

CRediT authorship contribution statement

Barbara Bellich: Visualization, Methodology, Investigation. **Michele Cacioppo:** Writing – original draft, Methodology, Investigation. **Rita De Zorzi:** Writing – original draft, Methodology, Investigation. **Roberto Rizzo:** Writing – original draft, Data curation, Conceptualization. **John W. Brady:** Supervision, Funding acquisition, Conceptualization. **Paola Cescutti:** Writing – review & editing, Writing – original draft, Supervision, Data curation, Conceptualization.

Declaration of competing interest

The authors declare that they have no conflicts of interest with the contents of this article.

Data availability

Data will be made available on request.

Acknowledgments

This work was supported by the National Institutes of Health (USA), (Grant Number GM123283).

Appendix A. Supplementary data

Supplementary data to this article can be found online at https://doi.org/10.1016/j.ijbiomac.2024.136222.

References

[1] H.C. Flemming, J. Wingender, U. Szewzyk, P. Steinberg, S.A. Rice, S. Kjelleberg, Biofilms: an emergent form of bacterial life, Nat. Rev. Microbiol. 14 (2016) 563–575, https://doi.org/10.1038/nrmicro.2016.94.
[2] S. Vani, K. Vadakkan, B. Mani, A narrative review on bacterial biofilm: its formation, clinical aspects and inhibition strategies, Futur. J. Pharm. Sci. 9 (2023) 50, https://doi.org/10.1186/s43094-023-00499-9.
[3] T. Tolker-Nielsen T, 2015. Biofilm development. Microbiol. Spectr. 3(2), MB-0001-2014. doi:https://doi.org/10.1128/microbiolspec.MB-0001-2014.
[4] K. Papenfort, B.L. Bassler, Quorum sensing signal-response systems in gram-negative bacteria, Nat. Rev. Microbiol. 14 (9) (2016) 576–588, https://doi.org/10.1038/nrmicro.2016.89.
[5] A. Dragoš, Á.T. Kovács, The peculiar functions of the bacterial extracellular matrix, Trends Microbiol. 25 (4) (2017) 257–266, https://doi.org/10.1016/j.tim.2016.12.010.
[6] D.G. Allison, The biofilm matrix, Biofouling 19 (2003) 139–150, https://doi.org/10.1080/0892701031000072190.
[7] B. Cuzzi, Y. Herasimenka, A. Silipo, R. Lanzetta, G. Liut, R. Rizzo, P. Cescutti, Versatility of the *Burkholderia cepacia* complex for the biosynthesis of exopolysaccharides: a comparative structural investigation, PloS One 9 (2014) e94372, https://doi.org/10.1371/journal.pone.0094372.
[8] S. Dolfi, A. Sveronis, A. Silipo, R. Rizzo, P. Cescutti, A novel rhamno-mannan exopolysaccharide isolated from biofilms of *Burkholderia multivorans* C1576, Carbohydr. Res. 411 (2015) 42–48, https://doi.org/10.1016/j.carres.2015.04.012.
[9] B. Bellich, I.A. Jou, C. Buriola, N. Ravenscroft, J. W. Brady J.W., M. Fazli, T. Tolker-Nielsen, R. Rizzo, P. Cescutti, 2021. The biofilm of *Burkholderia cenocepacia* H111 contains an exopolysaccharide composed of rhamnose and L-mannose: structural characterization and molecular modelling. Carbohydr. Res. 499, 108231. doi:https://doi.org/10.1016/j.carres.2020.108231.
[10] B. Bellich, I.A. Jou, M. Caterino, R. Rizzo, N. Ravenscroft, M. Fazli, T. Tolker-Nielsen, J.W. Brady, P. Cescutti, *Burkholderia cenocepacia* H111 produces a water-insoluble exopolysaccharide in biofilm: structural determination and molecular modelling, Int. J. Mol. Sci. 21 (2020) 1702–1714, https://doi.org/10.3390/ijms21051702.
[11] P. Drevinek, E. Mahenthiralingam, *Burkholderia cenocepacia* in cystic fibrosis: epidemiology and molecular mechanisms of virulence, Clin. Microbiol. Infect. 16 (7) (2010) 821–830, https://doi.org/10.1111/j.1469-0691.2010.03237.x.
[12] D. Chang, L. Sharma, C.S. Dela Cruz, D. Zhang, Clinical epidemiology, risk factors, and control strategies of *Klebsiella pneumoniae* infection, Front. Microbiol. 22 (12) (2021) 750662, https://doi.org/10.3389/fmicb.2021.750662.
[13] M.M. Kuttel, P. Cescutti, M. Distefano, R. Rizzo, Fluorescence and NMR spectroscopy together with molecular simulations reveal amphiphilic characteristics of a *Burkholderia* biofilm exopolysaccharide, J. Biol. Chem. 292 (2017) 11034–11042, https://doi.org/10.1074/jbc.M117.785048.
[14] B. Bellich, C. Lagatolla, R. Rizzo, M.M. D'Andrea, G.M. Rossolini, P. Cescutti, Determination of the capsular polysaccharide structure of the *Klebsiella pneumoniae* ST512 representative strain KPB-1 and assignments of the glycosyltransferases functions, Int. J. Biol. Macromol. 155 (2020) 315–323, https://doi.org/10.1016/j.ijbiomac.2020.03.196.
[15] B. Bellich, M. Distefano, Z. Syrgiannis, S. Bosi, F. Guida, R. Rizzo, J.W. Brady, P. Cescutti, The polysaccharide extracted from the biofilm of *Burkholderia multivorans* strain C1576 binds hydrophobic species and exhibits a compact 3D-structure, Int. J. Biol. Macromol. 136 (2019) 944–950, https://doi.org/10.1016/j.ijbiomac.2019.06.140.
[16] M. Cacioppo, R. De Zorzi, Z. Syrgiannis, B. Bellich, P. Bertoncin, I.A. Jou, J. W. Brady, R. Rizzo, P. Cescutti, Microscopy and modelling investigations on the morphology of the biofilm exopolysaccharide produced by *Burkholderia multivorans* strain C1576, Int. J. Biol. Macromol. 253 (2023) 127294, https://doi.org/10.1016/j.ijbiomac.2023.127294.
[17] Y. Deng, J. Wu, L. Eberl, L.H. Zhang, Structural and functional characterization of diffusible signal factor family quorum-sensing signals produced by members of the *Burkholderia cepacia* complex, Appl. Environ. Microbiol. 76 (14) (2010) 4675–4683, https://doi.org/10.1128/AEM.00480-10.
[18] S. Genin, T.P. Denny, Pathogenomics of the *Ralstonia solanacearum* species complex, Annu. Rev. Phytopathol. 50 (2012) 67–89, https://doi.org/10.1146/annurev-phyto-081211-173000.
[19] C.N.H. Marques, D.G. Davies, K. Sauer, Control of biofilms with the fatty acid signaling molecule *cis*-2-Decenoic acid, Pharmaceuticals 8 (2015) 816–835, https://doi.org/10.3390/ph8040816.
[20] E. Mahenthiralingam, T. Coenye, J.W. Chung, D.P. Speert, J.R.W. Govan, P. Taylor, P. Vandamme, Diagnostically and experimentally useful panel of strains from the *Burkholderia cepacia* complex, J. Clin. Microbiol. 38 (2000) 910–913, https://doi.org/10.1128/JCM.38.2.910-913.2000.
[21] M. Fazli, Y. McCarthy, M. Givskov, R.P. Ryan, T. Tolker-Nielsen, The exopolysaccharide gene cluster Bcam1330–Bcam1341 is involved in *Burkholderia cenocepacia* biofilm formation, and its expression is regulated by c-di-GMP and Bcam1349, MicrobiologyOpen 2 (2013) 105–122, https://doi.org/10.1002/mbo3.61.

[22] A. Carlier, K. Agnoli, G. Pessi, A. Suppiger, C. Jenul, N. Schmid, B. Tümmler, M. Pinto-Carbo, L. Eberl, Genome sequence of *Burkholderia cenocepacia* H111, a cystic fibrosis airway isolate, Genome Announc. 2 (2014) e00298-14, https://doi.org/10.1128/genomeA.00298-14.

[23] T.M. McIntire, D.A. Brant, Imaging of individual biopolymers and supramolecular assemblies using noncontact atomic force microscopy, Biopolymers 42 (1997) 133–146, https://doi.org/10.1002/(SICI)1097-0282(199708)42:2<133::AID-BIP3>3.0.CO;2-O.

[24] Y. Herasimenka, P. Cescutti, C.E. Sampaio Noguera, J.R. Ruggiero, R. Urbani, G. Impallomeni, F. Zanetti, S. Campidelli, M. Prato, R. Rizzo, Macromolecular properties of cepacian in water and dimethylsuphoxide, Carbohydr. Res. 343 (2008) 81–89, https://doi.org/10.1016/j.carres.2007.10.003.